Journal of Materials Chemistry A

PAPER

View Article Online
View Journal | View Issue

Cite this: J. Mater. Chem. A, 2015, 3, 12436

A hybrid physical–chemical deposition process at ultra-low temperatures for high-performance perovskite solar cells†

Yanke Peng,‡[a] Gaoshan Jing‡[a] and Tianhong Cui*[ab]

Received 7th March 2015
Accepted 30th April 2015

DOI: 10.1039/c5ta01730k

www.rsc.org/MaterialsA

The quality of a perovskite film will directly determine the performance and stability of the corresponding perovskite solar cell. High-quality and uniform $CH_3NH_3PbI_3$ films were synthesized by a new hybrid physical–chemical vapor deposition (HPCVD) process in a vacuum and isothermal environment. The reaction temperature can be accurately adjusted from 73 °C to 100 °C, with 73 °C as the lowest reaction temperature for a vapor based approach. $CH_3NH_3PbI_3$ solar cells with high performance were fabricated at 82 °C to achieve a high power conversion efficiency (PCE) up to 14.7%. The unsealed champion solar cell was tested for 31 days continuously, and its efficiency could maintain 12.1%, demonstrating high effectiveness of this HPCVD process.

Introduction

The power conversion efficiency (PCE) record of the hybrid inorganic–organic perovskite solar cell developed at research labs has soared from 3.8% to 20.1% in five years (2009–2014),[1,2] comparable to the PCEs of GaAs thin film and silicon based solar cells constructed with nanostructures to increase light collection efficiency through light trapping or concentration.[3–5] The next great challenge that global researchers are facing is to develop high-performance and stable perovskite solar cells in cost efficient ways, so that this technology can compete with commercially available thin film photovoltaic technologies for probable broad applications, *e.g.* CdTe based solar cells, which have the lowest production cost among all solar cells currently.[6]

Performance of a perovskite solar cell is highly determined by the crystalline quality of the perovskite thin film sandwiched between electron and hole transport layers in a typical perovskite solar cell structure, such as the size of perovskite grains and the uniformity of the thin films.[7–10] There are two major types of methods to synthesize perovskite films, solution based ("wet") and vapor based ("dry") methods. One key procedure to obtain high quality perovskite films is to optimize perovskite material reaction and crystallization rate. By using a two-step solution-based method, a high quality perovskite film is rarely obtained due to a high reaction rate between the solid PbI_2 precursor film and the high concentration CH_3NH_3I/2-propanol (IPA) solution.[11] To reduce the perovskite reaction rate, a two-step spin-coating procedure was introduced by spin coating the CH_3NH_3I/IPA solution with an optimized concentration on PbI_2 precursor thin films.[12] In a one step solution based method, additional chlorine based materials and procedures during spin coating are introduced to optimize the perovskite crystallization rate: (1) adding $PbCl_2$ (ref. 13) or CH_3NH_3Cl (ref. 14) into a perovskite solution for one-step spin coating; (2) dripping toluene when spin coating the perovskite solution,[8] and (3) adding argon flow during the solution spin-coating process to improve perovskite film quality.[15] Water vapor and oxygen in an ambient environment degenerate perovskite films so drastically that a nitrogen filled glove box was widely used to synthesize the perovskite material for solution based methods.[16,17] Nevertheless, it is still quite challenging to obtain high-quality, stable perovskite films using solution-based methods.

Perovskite thin films are synthesized by two solid precursors with a large difference in material properties. One is lead halide, an inorganic material with an appropriate evaporation temperature of about 320 °C, and the other is alkyl amino halide, an organic material with an appropriate temperature below 120 °C. Without proper gas precursors, the conventional CVD system is not suitable for synthesizing perovskite films without modifying system configuration and deposition procedures. A few vapor based methods using modified PVD or CVD systems were developed to synthesize high-quality perovskite films, including dual-source vapor deposition,[18,19] vapor assistant solution process (VASP),[9,20] and hybrid chemical vapor deposition.[21–24] By the dual-source vapor deposition method, a high-performance solar cell with 15.4% efficiency was fabricated when alkyl amino halide and lead halide were

[a]State Key Laboratory of Precision Measurement Technology and Instruments, Department of Precision Instruments, Tsinghua University, Beijing, 100084, China. E-mail: tcui@me.umn.edu

[b]Department of Mechanical Engineering, University of Minnesota, Minneapolis, Minnesota 55455, USA. Tel: +1-612-626-1636

† Electronic supplementary information (ESI) available: Photovoltaic parameters of solar cells structured from $CH_3NH_3PbI_3$ films by HPCVD at 73, 82, 90, and 100 °C. See DOI: 10.1039/c5ta01730k

‡ The first two authors contributed equally to this work.

evaporated simultaneously in a high vacuum chamber, and then deposited and reacted on a compact TiO_2/FTO substrate.[18] With the VASP method, uniform $CH_3NH_3PbI_3$ films with grain sizes as large as 500 nm and surface roughness as small as RMS 23.2 nm were synthesized in a glove box by reacting alkyl amino halide (*e.g.*, CH_3NH_3I) vapor with solid PbI_2 thin films. Corresponding perovskite solar cells exhibited high performance with 12.1% efficiency. Using a low pressure (0.3 Torr) VASP method, PbI_2/$PbCl_2$ mixed halide precursor films were annealed in CH_3NH_3I vapor at 120 °C to synthesize perovskite films and the PCE of the best solar cell was up to 16.8% (reverse scanning) and 15.4% (forward scanning).[20] Another promising method is to use the chemical vapor deposition method to synthesize perovskite films. High-quality perovskite nanoplatelets were grown on a muscovite mica surface by a hybrid CVD system with the electron diffusion length over 200 nm.[24] In a hybrid CVD method dual temperature zones were applied to synthesize perovskite films and to form a solar cell with an efficiency up to 11.8%.[23] In vapor based methods, the perovskite growth rate is determined by the vapor reaction process, such as reaction temperature, vapor pressure, and vacuum level. To date, these vapor based methods have not been widely adapted because such parameters were difficult to adjust independently and accurately for high-quality perovskite material synthesis.

Here, we introduce a new hybrid physical–chemical vapor deposition (HPCVD) method to synthesize high-quality perovskite films of $CH_3NH_3PbI_3$. Comparing to published vapor based methods, $CH_3NH_3PbI_3$ thin films were synthesized in a well-controlled vacuum and isothermal environment. Critical reaction parameters, including vapor pressure and reaction temperature, can be adjusted accurately to further improve perovskite film quality. As shown in Fig. 1, PbI_2 solid thin film precursor (on mesoporous TiO_2 (m-TiO_2)/compact TiO_2 (c-TiO_2)/FTO substrates) and CH_3NH_3I crystal solid precursor were placed into a quartz boat and then put inside an isothermal vacuum quartz tube. By heating up to a certain temperature, the evaporated CH_3NH_3I vapor reacted with the solid PbI_2 films to synthesize uniform $CH_3NH_3PbI_3$ thin films. In this method, a vacuum level of 2 mTorr is maintained to reduce perovskite film defects. Due to the easy sublimation of organic precursor CH_3NH_3I heated at 70 °C or above, the pressure in the quartz tube was about 15–30 mTorr under vacuum pumping. With two quartz blocks at the ends of the quartz tube, CH_3NH_3I vapor pressure on the PbI_2 film surface can be maintained in a "quasi" stable status during vacuum pumping. Meanwhile, the pressure can be changed by adjusting the placement configuration between these two precursor materials. A constant reaction temperature between 73 °C and 100 °C was set to synthesize high-quality $CH_3NH_3PbI_3$ thin films, with 73 °C being the lowest temperature to synthesize perovskite films so far as we know. Highly uniform perovskite films were synthesized, and high PCEs of up to 14.7% (reverse scanning) and 11.5% (forward scanning) at 82 °C were achieved for these solar cells. The unsealed champion solar cell was tested for 31 days continuously, and its reverse scan mode efficiency can still maintain 12.1%, demonstrating the effectiveness and stability of this new HPCVD method. This vacuum and vapor based method is compatible with conventional semiconductor fabrication methods, and high-quality perovskite films can be achieved through a delicate process control. Eventually, perovskite based solar cells could be mass produced at a low cost for large-scale applications by this new method.

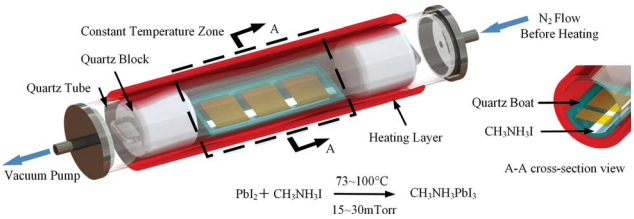

Fig. 1 Schematic diagram of a hybrid physical–chemical vapor deposition (HPCVD) method for synthesizing perovskite ($CH_3NH_3PbI_3$) films.

Experimental

Synthesis of CH_3NH_3I

Methylamine (27.86 mL, 40% in methanol, Sigma) and hydroiodic acid (30 mL, 57 wt% in water, Aldrich) were mixed at 0 °C and stirred for 2 h. The precipitate was recovered by evaporation at 50 °C for 1 h. The product was washed with diethyl ether three times and finally dried at 60 °C in a vacuum oven for 24 h.

Substrate preparation

FTO-coated glass sheets (20 × 20 mm, Tec15, Pilkington, St Helens, United Kingdom) were patterned by a laser cutter. These sheets were then cleaned by ultra-sonication in de-ionized (DI) water, ethanol, acetone, isopropyl alcohol (IPA) and DI water sequentially for 15 min, respectively. Finally, they were treated in an oxygen plasma asher (PDC-32G-2, Henniker Plasma, Warrington, UK) for 15 min to remove the organic residues on the surfaces.

Solar cell fabrication

An acidic solution of titanium isopropoxide[18] (Sigma-Aldrich, 99.999%, St. Louis, USA) in ethanol was spin-coated onto the clean FTO sheet at 2000 rpm for 40 s, and then sintered at 500 °C for 30 min to form a compact TiO_2 layer with a thickness of 20–40 nm. The mesoporous TiO_2 layer was deposited by spin coating at 5000 rpm for 15 s using a commercial TiO_2 paste (NJU-SR, Sunlaite, Suzhou, China) diluted in ethanol (1 : 4, weight ratio). After baking at 120 °C for 10 min, the mesoporous TiO_2 films were sintered at 500 °C for 30 min and then cooled to room temperature. The substrates were treated in a 50 mM aqueous solution of $TiCl_4$ for 30 min at 70 °C, rinsed with DI water and ethanol and dried at 500 °C for 30 min. PbI_2 was dissolved in *N*,*N*-dimethylformamide (DMF, Sigma, St. Louis, USA) at a concentration of 461 mg mL^{-1} under stirring at 70 °C. The solution was kept at 70 °C during the whole procedure and

TiO_2 substrates were pre-heated at 70 °C. 80 μL of PbI_2/DMF solution was spin-coated on each substrate at 4500 rpm for 20 s in ambient air with the relative humidity below 30%. After heating at 70 °C in the air for 30 min, the PbI_2 substrates were laid upon the CH_3NH_3I powder with PbI_2 side back to the powder in a quartz boat. Then, the boat filled with CH_3NH_3I powder and PbI_2 substrates was put into the quartz tube. After flanges were mounted on the tube, the vacuum in the tube was pumped to 10 mTorr. Then, 50 sccm nitrogen flow was input into the tube to clean the inner surface for 20 min. When the valve of the nitrogen flow was shut down, the vacuum in the quartz tube could increase to 2 mTorr. 80, 90, 100, and 110 °C were set as the heating temperatures in the furnace control program, but the real temperatures in the tube were 73, 82, 90, and 100 °C respectively, which were calibrated by a wireless PT1000 temperature recorder (TP-1000-W1, A-Volt Co., Ltd, Beijing, China) laid in the vacuum quartz tube during the heating procedures. The actual temperature curve inside the quartz tube is shown in Fig. S1.† After three hours' reaction in the quartz tube, the perovskite films were annealed at 100 °C for 10 min at a relative humidity of 30 ± 5% in the ambient environment by following a published procedure for a high efficiency solar cell fabrication method.[10,25] Then 150 nm spiro-OMeTAD was spin-coated onto the perovskite films at 4000 rpm according to previously reported methods.[12] Finally, a 60 nm gold electrode was then deposited by E-beam evaporation. The active area of a typical solar cell was 0.16 cm^2.

Characterization

A field-emission scanning electron microscope (FE-SEM, Zeiss Merlin) was used to investigate the surface and cross-sectional morphology of the perovskite solar cells. Current density–voltage (J–V) curves were measured using an Agilent B1500A Semiconductor Device Parameter Analyser, which can measure the current–voltage curves of samples at the pA level. The measurements were carried out under AM1.5G illumination at 100 mW cm^{-2} provided by a Newport ABB (94021A) solar simulator in ambient air. Light intensity was calibrated with a Newport calibrated mono-Si reference cell (Newport calibration cert. #0702). A testing mask was used during the measurements with an active area of 0.09 cm^2. The J–V curves were obtained in the air (1.2 V to −0.1 V to 1.2 V) with the step size of 20 mV. The delay time at every measurement point is 50 ms. Incident Photon to Current Conversion Efficiencies (IPCE) were measured using an Oriel IQE 200 equipment.

Results and discussion

In the HPCVD method, two critical parameters, CH_3NH_3I vapor pressure and reaction temperature, can be delicately adjusted to synthesize high-quality $CH_3NH_3PbI_3$ films. As shown in Fig. 1, a vacuum pump was kept running and the CH_3NH_3I was kept sublimating during the process to prevent from leakage contamination through an ambient environment, so that the pressure inside the quartz tube is not of the same value. The

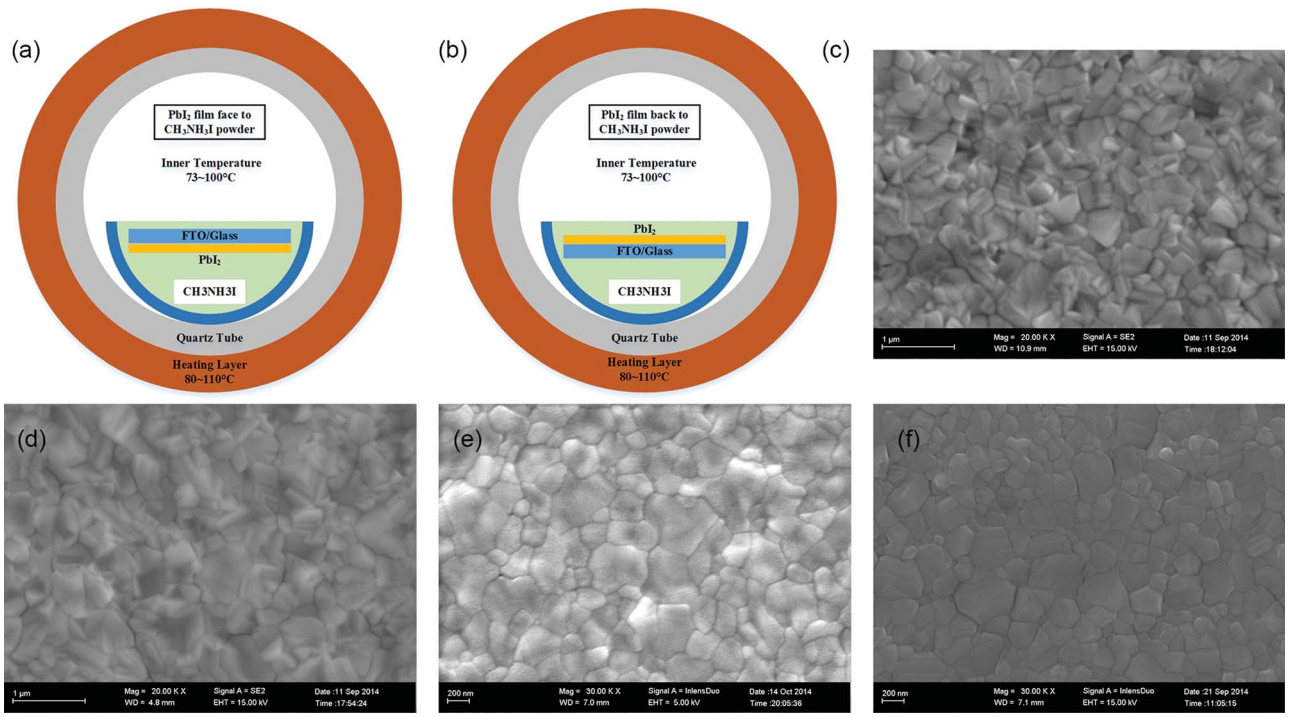

Fig. 2 Schematic diagrams of two precursor material (PbI_2 thin film and CH_3NH_3I powder crystal) placement configurations in the HPCVD process: (a) "face to face" configuration and (b) "back to face" configuration. Top view scanning electron microscopy (SEM) images of $CH_3NH_3PbI_3$ films formed by HPCVD at 100 °C: (c) "face to face" configuration before annealing; (d) "face to face" configuration after annealing at 100 °C for 10 min; (e) "back to face" configuration before annealing; and (f) "back to face" configuration after annealing at 100 °C for 10 min in ambient air under a relative humidity (RH) of 30 ± 5%.

highest pressure would exist around the quartz boat containing the CH_3NH_3I precursor crystal, which is close to the CH_3NH_3I vapor pressure at specific reaction temperature. Meanwhile, there would be the lowest pressure at the end of the quartz tube (equal to 2 mTorr). Because of the existence of two quartz blocks, the pressure gradient profile inside the tube should be maintained in a stable state without vapor convection turbulence. To demonstrate this hypothesis, we arranged two precursor materials in two placement configurations shown in Fig. 2a and b: one is "face to face" and the other is "back to face". CH_3NH_3I vapor pressure on the PbI_2 surface in the "face to face" configuration should be larger than that of "back to face" due to the blockage by the FTO substrate. Therefore, $CH_3NH_3PbI_3$ reaction in the "back to face" configuration should have a slower reaction rate than that of "face to face". As shown in Fig. 2c and e, a typical $CH_3NH_3PbI_3$ film synthesized in the "back to face" configuration is more uniform than its counterpart in the "face to face" configuration, probably because of the lower reaction rate. The surface profile difference became more apparent after the post-thermal annealing process at 100 °C for 10 min in ambient air under a relative humidity of 30 ± 5%, as shown in Fig. 2d and f. To obtain a $CH_3NH_3PbI_3$ film with better surface uniformity, we chose the "back to face" configuration in the HPCVD process. XRD spectra of the HPCVD perovskite films[26] show strong peaks at 14.18°, 28.52°, and 31.96°, corresponding to (110), (220), and (310) Miller indices of $CH_3NH_3PbI_3$ perovskite crystals. Compared with the XRD spectra of the perovskite film prepared by the traditional two-step solution method,[11] the relative heights and the full widths at half maximum (FWHM) of these peaks exhibit a better crystalline quality of HPCVD perovskite films. It should be noted that the emergence of a peak at 12.65° after the post-annealing process could have resulted from self-induced passivation of PbI_2 on perovskite grain structure surfaces, which could improve performance of the solar cells.[10,25] Besides CH_3NH_3I vapor pressure, reaction temperature (73 °C, 82 °C, 90 °C, and 100 °C) can be accurately adjusted to synthesize perovskite films. Uniform $CH_3NH_3PbI_3$ films can be obtained at 73 °C, which is the lowest reaction temperature for vapor based methods (Fig. 3). Comparing two films shown in Fig. 2e and 3a, larger crystalline size and more uniform surface were likely to be achieved at high reaction temperatures.

Efficiency statistics of solar cells obtained with $CH_3NH_3PbI_3$ films constructed by the HPCVD method at 73 °C, 82 °C, 90 °C and 100 °C are shown in Fig. 4. Detailed information about these solar cells is reported in the ESI.† Though the solar cell with the best performance (champion cell, PCE: 14.7% (reverse scanning mode) and 11.5% (forward scanning mode)) was obtained at 82 °C, devices obtained at 73 °C had the smallest PCE standard deviation compared to that of devices obtained at 82 °C, 90 °C and 100 °C shown in Table 1. The reason may be that the pressure gradient profile at 73 °C is smaller than that at 82 °C, 90 °C and 100 °C, and $CH_3NH_3PbI_3$ films were synthesized in a relative "quasi constant pressure" environment.

High performance $CH_3NH_3PbI_3$ solar cells were obtained by the HPCVD method at an ultra-low temperature of 73 °C. An SEM cross-sectional image of the gold/spiro-OMeTAD/$CH_3NH_3PbI_3$/m-TiO_2/c-TiO_2/FTO perovskite solar cell is shown in Fig. 5a. A uniform $CH_3NH_3PbI_3$ film about 250 nm thick was sandwiched between the hole transport layer (spiro-OMeTAD) and the electron transport layer (m-TiO_2). As shown in Fig. 5b, the best device obtained by HPCVD at 73 °C exhibits great performance, with reverse scan: J_{SC} = 22.63 mA cm^{-2}, V_{OC} = 1.05 V, filling factor (FF) = 60%, PCE = 14.1%; and forward scan: J_{SC} = 22.81 mA cm^{-2}, V_{OC} = 1.02 V, filling factor (FF) = 49%, PCE = 11.2%. The external quantum efficiency (EQE) spectrum is shown in Fig. 5c.

Integrating the overlap of the EQE spectrum with the AM1.5G solar photon flux yields a current density of 19.8 mA cm^{-2}, lower than the J_{SC} from the *J–V* curve. This probably could be attributed to the surface trap of the TiO_2 transport layer reported previously.

Compared to existing vapor based methods,[9,18–24] high performance perovskite solar cells by HPCVD were achieved under an ultra-low temperature of 73 °C. Meanwhile, a lead precursor cannot be fully converted into a perovskite material at an annealing temperature of 100 °C for LP-VASP[20] and a perovskite film was synthesized at 150 °C using VASP.[9] It could be the maintained high vacuum level (2 mTorr) prior to the HPCVD process that leads to such a low synthesis temperature. Theoretically, these vapor based processes can be divided into three sequential processes: (1) physical vapor deposition (PVD)

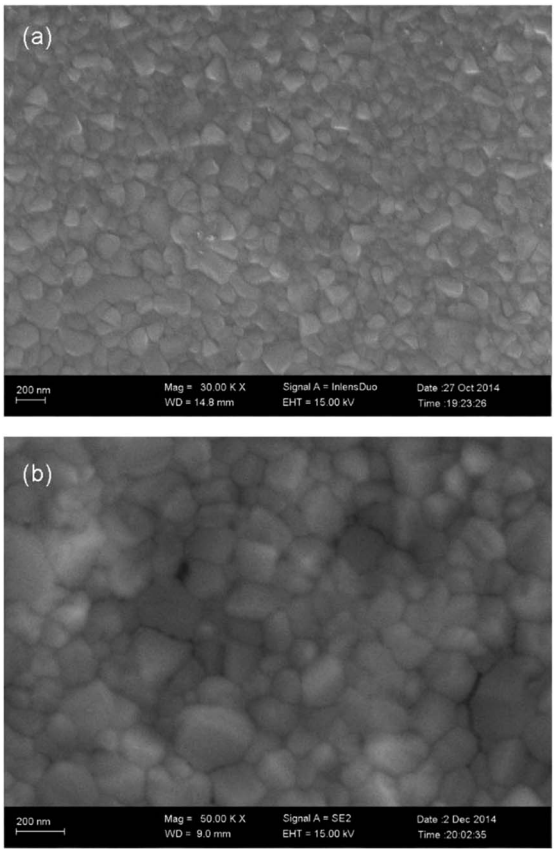

Fig. 3 Top view SEM images of a $CH_3NH_3PbI_3$ film formed by HPCVD at 73 °C (a) before and (b) after annealing at 100 °C for 10 min in ambient air under a relative humidity of 30 ± 5%.

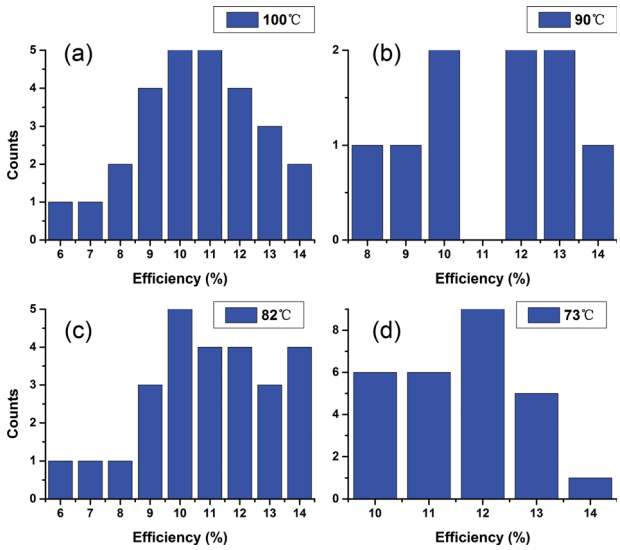

Fig. 4 Power conversion efficiency (PCE) statistics of perovskite solar cells with $CH_3NH_3PbI_3$ films synthesized at different reaction temperatures.

process: CH_3NH_3I powder is evaporated and CH_3NH_3I vapor arrives onto a solid substrate with a perovskite film synthesized beforehand, with a PbI_2 precursor film underneath; (2) gas phase/solid phase transportation process: CH_3NH_3I vapor diffuses through the solid perovskite film and onto the PbI_2 precursor film surface; (3) surface reaction process: CH_3NH_3I vapor reacts with the PbI_2 precursor film, and thickness of the perovskite layer increases. For the PVD process determined by pressure and temperature, the evaporation rate of CH_3NH_3I vapor can be described by the following formula:[27]

$$\Gamma = 5.84 \times 10^{-2} \left(\frac{M}{T}\right)^{\frac{1}{2}} (P_e - P_h) \quad \text{g cm}^{-2}\ \text{s}^{-1} \qquad (1)$$

where M is the molecular weight of CH_3NH_3I, T is the temperature, P_e is the vapor pressure of CH_3NH_3I at specific temperature and P_h is the chamber pressure.

At a certain temperature, vapor pressure of CH_3NH_3I (P_e) is a constant in an equilibrium state. With higher chamber pressure (P_h), the lower evaporation rate can be achieved for CH_3NH_3I vapor. The lower evaporation rate can lead to slower CH_3NH_3I vapor diffusion rate and smaller surface reaction rate. Eventually, when thickness of PbI_2 film is over a certain threshold, full conversion of the precursor film is not feasible. For VASP, LP-VASP and HPCVD methods, P_h values are 760 Torr,[9] 0.3 Torr [20] and 2 mTorr, respectively, which may explain why perovskite films 200–300 nm thick should be synthesized at 150 °C by VASP, 120 °C by LP-VASP, while 73 °C (even for the "back to face" configuration with a slower growth rate) by HPCVD. In addition, the PbI_2 precursor film could not be fully converted

Table 1 PCE statistics of perovskite solar cells with $CH_3NH_3PbI_3$ films synthesized at different reaction temperatures

Group	No. total	Mean	Standard deviation	Min.	Median	Max.
100 °C	27	11.1%	2.07%	6.2%	11.5%	14.2%
90 °C	9	11.7%	1.96%	8.7%	12.5%	14.1%
82 °C	26	11.4%	2.10%	6.9%	11.3%	14.7%
73 °C	27	12.0%	1.12%	10.1%	12.3%	14.1%

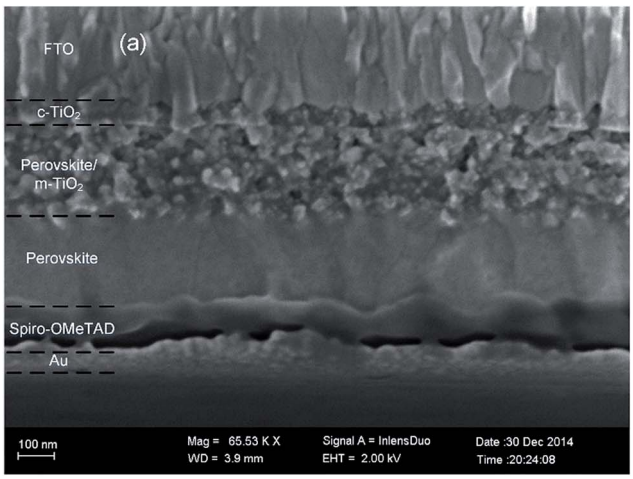

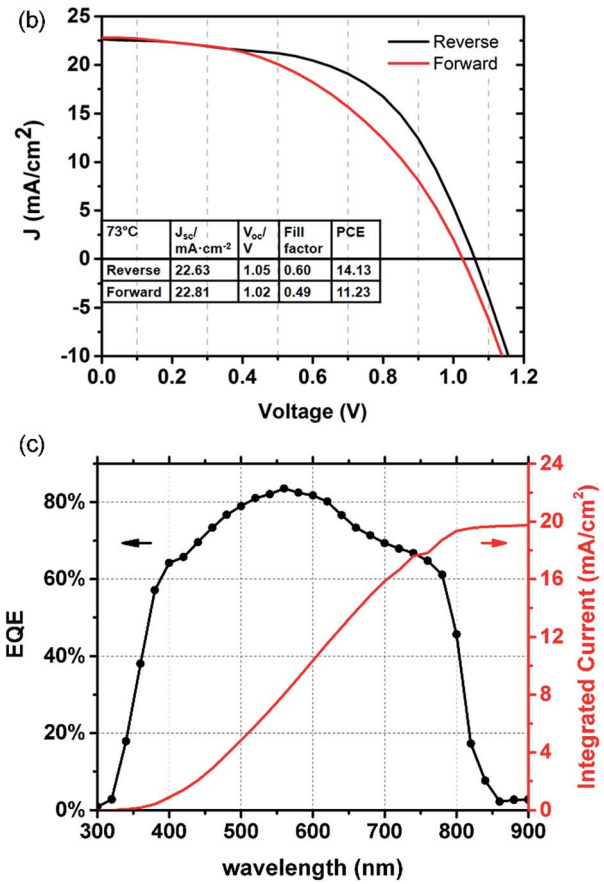

Fig. 5 (a) Cross-sectional view SEM image of a completed solar cell constructed from a HPCVD $CH_3NH_3PbI_3$ film about 250 nm thick at 73 °C for 150 min. (b) Current–density *vs.* voltage curves of the best performing solar cell fabricated by the same process measured under simulated AM1.5 sunlight of 100 mW cm^{-2} irradiance. (c) External quantum efficiency (EQE) spectrum of this device with an integrated current density of 19.8 mA cm^{-2}.

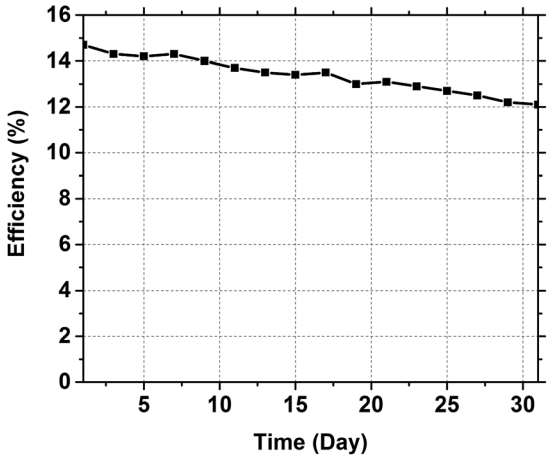

Fig. 6 PCE decay curve of the champion perovskite solar cell (reverse scan mode: 14.7%). The unsealed champion cell was tested every day in the ambient environment with the relative humidity below 30% to characterize its long-term stability. After 31 days' testing, its efficiency maintained 12.1% (reverse scan mode). The device was stored in a vessel with phosphorous oxide as the desiccant.

into a perovskite film after twelve hours of reaction at 60 °C by HPCVD. Further investigation on HPCVD's reaction kinetics is underway.

Finally, a long-term stability test was done for the champion cell obtained at 82 °C. The unsealed champion solar cell was tested for 31 days continuously, and its reverse scan mode efficiency could still maintain 81% of its initial efficiency (12.1% *vs.* 14.7%) (Fig. 6), demonstrating the effectiveness and stability of this new HPCVD method, compared to the reported unsealed perovskite solar cell which decayed rapidly during the storage period.[10] The relatively high performance with long-term stability may contribute to the low vacuum level environment for synthesizing perovskite materials. Inside the quartz tube, concentrations of corrosive molecules, such as water vapor, oxygen and organic chemicals, are much lower than those in an ambient environment or a glove box resulting in much less corrosive molecules being trapped inside the perovskite material. As the perovskite solar cells were tested or stored in atmosphere, water vapor and oxygen in the ambient environment would gradually diffuse into the perovskite material causing slow degradation of the solar cell's performance for a testing period of 31 days. However, due to very few corrosive molecules being trapped into the perovskite material synthesized in a high vacuum, the performance decay rate of the perovskite solar cell by HPCVD was much slower than that of perovskite solar cells fabricated in ambient air. Further investigation on perovskite film defects is underway.

Conclusion

In summary, high-quality $CH_3NH_3PbI_3$ films and corresponding solar cells were prepared by a new hybrid physical–chemical vapor deposition (HPCVD). In this method, vapor pressure can be adjusted by changing the configuration of the PbI_2 substrate. The reaction temperature can be accurately adjusted from 73 to 100 °C. By optimizing these reaction parameters, high performance $CH_3NH_3PbI_3$ solar cells were fabricated to achieve a high power conversion efficiency up to 14.7%. The unsealed champion solar cell was tested for 31 days continuously, and its efficiency (reverse scan mode) still maintained 12.1%. High stability of such devices could be due to the highly uniform perovskite film synthesized in a vacuum environment, free of water vapor/oxygen contamination. The slow reaction rate to synthesize a dense material could further increase the stability of the devices. In future, parameters of this HPCVD method (vacuum level, reaction temperature, reaction time, *etc.*) could be further optimized respectively to achieve solar devices with better performance. Eventually, perovskite solar cells could be mass produced at a low cost for large-scale applications by this new method.

Acknowledgements

This work was financially supported by the International Science and Technology Cooperation Program of Ministry of Science and Technology of the People's Republic of China (Grant no. 2013DFA51800).

Notes and references

1 A. Kojima, K. Teshima, Y. Shirai and T. Miyasaka, *J. Am. Chem. Soc.*, 2009, **131**, 6050–6051.
2 http://www.nrel.gov/ncpv/images/efficiency_chart.jpg, accessed 02-04, 2015.
3 J. Yang, F. Luo, T. S. Kao, X. Li, G. W. Ho, J. Teng, X. Luo and M. Hong, *Light: Sci. Appl.*, 2014, **3**, e185.
4 M. Memarian and G. V. Eleftheriades, *Light: Sci. Appl.*, 2013, **2**, e114.
5 E. D. Kosten, J. H. Atwater, J. Parsons, A. Polman and H. A. Atwater, *Light: Sci. Appl.*, 2013, **2**, e45.
6 Advance PV modules, http://www.firstsolar.com/en/technologies-and-capabilities/pv-modules, accessed Mar. 22, 2015.
7 C. Wehrenfennig, M. Liu, H. J. Snaith, M. B. Johnston and I. Herz, *Energy Environ. Sci.*, 2014, **7**, 2269–2275.
8 N. J. Jeon, J. H. Noh, Y. C. Kim, W. S. Yang, S. Ryu and S. I. Seok, *Nat. Mater.*, 2014, **13**, 897–903.
9 Q. Chen, H. Zhou, Z. Hong, S. Luo, H. S. Duan, H. H. Wang, Y. Liu, G. Li and Y. Yang, *J. Am. Chem. Soc.*, 2014, **136**, 622–625.
10 H. Zhou, Q. Chen, G. Li, S. Luo, T. B. Song, H. S. Duan, Z. Hong, J. You, Y. Liu and Y. Yang, *Science*, 2014, **345**, 542–546.
11 J. Burschka, N. Pellet, S. J. Moon, R. Humphry-Baker, P. Gao, M. K. Nazeeruddin and M. Gratzel, *Nature*, 2013, **499**, 316–319.
12 J. H. Im, I. H. Jang, N. Pellet, M. Gratzel and N. G. Park, *Nat. Nanotechnol.*, 2014, **9**, 927–932.
13 M. M. Lee, J. Teuscher, T. Miyasaka, T. N. Murakami and H. J. Snaith, *Science*, 2012, **338**, 643–647.
14 Y. Zhao and K. Zhu, *J. Phys. Chem. C*, 2014, **118**, 9412–9418.

15 F. Huang, Y. Dkhissi, W. Huang, M. Xiao, I. Benesperi, S. Rubanov, Y. Zhu, X. Lin, L. Jiang, Y. Zhou, A. Gray-Weale, J. Etheridge, C. R. McNeill, R. A. Caruso, U. Bach, L. Spiccia and Y.-B. Cheng, *Nano Energy*, 2014, **10**, 10–18.
16 W. Li, H. Dong, L. Wang, N. Li, X. Guo, J. Li and Y. Qiu, *J. Mater. Chem. A*, 2014, **2**, 13587–13592.
17 G. Niu, X. Guo and L. Wang, *J. Mater. Chem. A*, 2015, **3**, 8970–8980.
18 M. Liu, M. B. Johnston and H. J. Snaith, *Nature*, 2013, **501**, 395–398.
19 B.-S. Kim, T.-M. Kim, M.-S. Choi, H.-S. Shim and J.-J. Kim, *Org. Electron.*, 2015, **17**, 102–106.
20 Y. Li, J. K. Cooper, R. Buonsanti, C. Giannini, Y. Liu, F. M. Toma and I. D. Sharp, *J. Phys. Chem. Lett.*, 2015, **6**, 493–499.
21 D. J. Lewis and P. O'Brien, *Chem. Commun.*, 2014, **50**, 6319–6321.
22 P. Luo, Z. Liu, W. Xia, C. Yuan, J. Cheng and Y. Lu, *ACS Appl. Mater. Interfaces*, 2015, **7**, 2708–2714.
23 M. R. Leyden, L. K. Ono, S. R. Raga, Y. Kato, S. Wang and Y. Qi, *J. Mater. Chem. A*, 2014, **2**, 18742–18745.
24 S. T. Ha, X. F. Liu, Q. Zhang, D. Giovanni, T. C. Sum and Q. H. Xiong, *Adv. Opt. Mater.*, 2014, **2**, 838–844.
25 J. You, Y. M. Yang, Z. Hong, T.-B. Song, L. Meng, Y. Liu, C. Jiang, H. Zhou, W.-H. Chang and G. Li, *Appl. Phys. Lett.*, 2014, **105**, 183902.
26 Y. Peng, G. Jing and T. Cui, in *MRS Sring 2015*, San Francisco, 2015.
27 O. Milton, *Materials Science of Thin Films*, Academic Press, San Diego, 2002.